Astronomy & Astrophysics manuscript no. aa1011proofs July 30, 2004
(DOI: will be inserted by hand later)

A spectroscopic atlas of the HgMn star HD 175640 (B9 V) $\lambda\lambda$ 3040-10000 Å*

F. Castelli[1,2] and S. Hubrig[3]

[1] Istituto di Astrofisica Spaziale e Fisica Cosmica, CNR, Via del Fosso del Cavaliere, I-00133 Roma, Italy
[2] Osservatorio Astronomico di Trieste, Via G.B. Tiepolo 11, Trieste, Italy, e-mail: castelli@ts.astro.it
[3] European Southern Observatory, Casilla 19001, Santiago 19, Chile, e-mail: shubrig@eso.org

Received .... ; accepted ....

Abstract. We present a high resolution spectral atlas of the HgMn star HD 175640 covering the 3040−10000 Å region. UVES spectra observed with 90000−110000 resolving power and signal to noise ratio ranging from 200 to 400 are compared with a synthetic spectrum computed with the SYNTHE code (Kurucz 1993b). The model atmosphere is an ATLAS12 model (Kurucz 1997) with parameters $T_{\rm eff}$=12000 K, log g=3.95, ξ=0 km s^{-1}. The stellar individual abundances in ATLAS12 were derived from an iterative procedure. The starting atomic line lists downloaded from the Kurucz website have been improved and extended by examining different sources in the literature and by comparing the computed profiles with the observed spectrum. The high quality of the data allowed us to study the isotopic and hyperfine structure for several lines of Mn II, Ga II, Ba II, Pt II, Hg I, and Hg II. Numerous weak emission lines from Cr II and Ti II have been identified in the red part of the spectrum, starting at $\approx \lambda$ 5847 Å. Two emission lines of C I (mult. 10, mult. 9) have been observed for the first time. All Cr II and Ti II emission lines originate from the high excitation states ($\chi_{low} > \sim$ 89000 cm^{-1} for Cr II and $\chi_{low} > \sim$ 62000 cm^{-1} for Ti II) with large transition probabilities (log $gf > -1.00$). The synthetic spectrum superimposed on the observed spectrum as well as the adopted improved atomic line lists are available at http://wwwuser.oat.ts.astro.it/castelli/stars.html. An extended discussion on each identified ion and related atomic data is available both on the quoted website and in an electronic Appendix to the paper.

Key words. stars:atmospheres; physical data and processes: atomic processes, atomic data; stars:abundances; stars:chemically peculiar; stars:individual (HR 7143)

1. Introduction

HD 175640 (HR 7143) is to a large extent representative of the HgMn stars, which constitute a well defined subgroup of chemically peculiar (CP) stars of late B spectral types in the temperature range 10000–14000 K. The most distinctive features are extreme atmospheric overabundances of Hg (up to 6 dex) and of Mn (up to 3 dex).

In the present study we undertook a detailed spectroscopic analysis of UVES spectra of HD 175640 in the whole region 3040-10000 Å. The high quality of the UV-Visual Echelle Spectrograph UVES at the 8 m UT2 telescope, its high resolution (R=90000−110000) and high signal-to-noise ratio (200-400), the large wavelength coverage, the low $v \sin i$ (2.5 km s^{-1}) of HD 175640 and its nature as a single star, led us to compute a synthetic spectrum for the whole observed interval. We used Kurucz codes and Kurucz line lists that we modified and implemented as explained in Sect. 4. The final results, which are available on our website[1], are the plots of the superimposed observed and synthetic spectra supplied with the line identifications as well as the modified Kurucz line lists that we adopted for the computations. An extended discussion of each ion analyzed during the preparation of the atlas is available in the electronic Appendix A of the paper.

The atlas of HD 175640 increases the number of those already published in a similar form. They are the o Peg atlas in the region $\lambda\lambda$3826−4882 Å (Gulliver et al. 2004) and the Deneb atlas in the region $\lambda\lambda$3825−5212 Å (Albayrak et al. 2003). In analogy with the two atlases quoted above the present one should also provide useful guidance for studies of other stars with similar spectral type. We wish to point out the much larger wavelength coverage (3040−10000 Å) of our atlas.

Compiling the atlas has required an abundance analysis for the 48 ions listed in Table 1 to which 9 more ions with dubious identifications or with no measurable lines

Send offprint requests to: F. Castelli

* Based on observations obtained at the European Southern Observatory, Paranal, Chile (ESO program No. 67.D-0579)

[1] http://wwwuser.oat.ts.astro.it/castelli/stars.html

can be added. They are B II, O II, S I, Zn I, Zn II, Ga I, As II, Ce II, and Ce III. Previous abundance determinations based on a few selected lines are those of Sadakane et al. (1985) for Be II, B II; Dworetsky & Buday (2000) for Ne I; Smith (1993) for Mg, Al, Si; Smith & Dworetsky (1993) and Jomaron et al. (1999) for Cr II, Mn II, Fe II, Co II, Ni II; Sadakane et al. (1988) and Smith (1996) for Cu II, Zn II; Smith (1996) and Dworetsky et al. (1998) for Ga II; Smith (1997) and Dolk et al. (2003) for Hg I, Hg II. We therefore extended the abundance analysis to more elements than those previously examined for this star.

The presence of emission lines was discovered for the first time in this star by Wahlgren & Hubrig (2000) in spectra observed in the intervals 6005-6095 Å and 6105-6190 Å. While most of them were identified as Ti II and Cr II lines, others could not be classified. In this paper we extended the search for the presence of emission lines to a larger wavelength interval than that explored by Wahlgren & Hubrig (2000). The nature of these emission lines remains unclear. A systematic investigation of the emission lines and the production of identification line lists in stars with different stellar parameters such as effective temperature, gravity, chemical composition, magnetic field strength, and rotational velocity would allow us to put tighter constraints on the modelling of the origin of emission lines in the HgMn, He-weak and PGa stars. Because the emission lines may be correlated with abundance stratification (Sigut 2001), UVES spectra also present an excellent opportunity to further investigate the vertical stratification of different chemical elements through the determination of the abundances from lines of the same ions formed on either side of the Balmer jump. For Ca II, Sc II, Ti II, Cr I, Cr II, Mn I, Fe I, Ni II, Y II, Zr II, and Yb II we compared abundances from lines lying shortward and longward of the Balmer discontinuity. Savanov & Hubrig (2003) already discussed the presence of Cr stratification in HD 175640 by analyzing Cr II lines on the wings of Hβ.

2. Observations

The spectrum of HD 175640 was recorded on June 13, 2001 at ESO with the VLT UV-Visual Echelle Spectrograph UVES at UT2. We used the UVES DIC1 and DIC2 standard settings covering the spectral range from 3030 Å to 10000 Å. The slit width was set to $0\farcs3$ for the red arm, corresponding to a resolving power of $\lambda/\Delta\lambda \approx 1.1 \times 10^5$. For the blue arm, we used a slit width of $0\farcs4$ to achieve a resolving power of $\approx 0.9 \times 10^5$. The spectra were reduced by the UVES pipeline Data Reduction Software (version 1.4.0), which is an evolved version of the ECHELLE context of MIDAS. The manual for the UVES pipeline can be found on the ESO web page[2]. The signal-to-noise ratios of the resulting UVES spectra are very high, ranging from 200 in the near UV to 400 in the visual region.

[2] http://www.eso.org/observing/dfo/quality/UVES/pipeline/pipe_gen.html

There are two gaps in the observed range at $\lambda\lambda$ 5759−5835 Å and 8519−8656 Å, which are caused by the physical gap between the two detector chips of the red CCD mosaic. Furthermore, the $\lambda\lambda$ 9074−9098 Å range cannot be used, as the spectrum quality is poor in this interval. The observed spectrum was shifted in wavelength in order to be superimposed on the computed spectrum. The shift ranges from 33.5 km s^{-1} in the ultraviolet to 34.5 km s^{-1} in the red, indicating an uncertainty of about 1.0 km s^{-1} in the wavelength calibration.

When the continuum was drawn in the spectrum reduced with the UVES pipeline, we noticed strong distortions, mostly in the ultraviolet, conspicuous jumps corresponding to the boundaries of the orders, and several spurious absorptions. Therefore we renormalised the unmerged spectra order by order from 3040 Å to 7000 Å. For λ>7000 Å, we adopted for the analysis the spectrum reduced with the UVES pipeline owing to the large undulations affecting the order by order spectra. As a consequence there are jumps in the red spectrum which modify the lines lying just where the jump occurs, as for instance Mn II at 8784 Å. There are also jumps at 8776.5 Å and 9316 Å, which could be confused with He I 8776.77 Å and with an emission line, respectively. Another jump occurs at 9038.3 Å.

The continuum was subjectively drawn by connecting the highest points of the spectrum by a straight line. When needed, it was then adjusted in steps of 6 Å intervals with the help of the synthetic spectrum. The continuous level just longward of the Balmer and Paschen discontinuities is highly uncertain. It was also very difficult to drawn it at the position of the Balmer and Paschen lines owing to the jumps and distortions of the échelle spectra. For this reason we did not use hydrogen lines for the analysis.

Equivalent widths were measured in the spectra by direct integration of the line profiles with the trapezium rule. A suitable number of points, which depends on the profile shape and intensity, was adopted for each measurament.

3. The Synthetic Spectrum

The synthetic spectrum was computed with the SYNTHE code (Kurucz 1993b) and with an opacity sampling ATLAS12 model (Kurucz 1997) computed for the individual abundances of the star.

Stellar parameters have been previously determined by Hubrig, Castelli & Wahlgren (1999) from Strömgren photometry and high resolution spectra in the framework of a spectroscopic search for magnetic fields in HgMn stars. We adopted the same values for the present analysis, namely $T_{\rm eff}$=12000 K, log g=3.95, microturbulent velocity ξ=0 km sec^{-1} and rotational velocity $v\sin i$=2.5 km s^{-1}. Although Hubrig & Castelli (2001) suggested the possible presence of a weak variable magnetic field in this star, we did not consider any Zeeman effect in the computed spectrum. The spectrum was broadened for $v\sin i$=2.5 km s^{-1} and for a gaussian instrumental profile with resolving power 90000 shortward of the Balmer discontinuity and 110000 longward of the Balmer discontinuity.

The final synthetic spectrum is the result of an iterative procedure. An opacity distribution function ATLAS9 (Kurucz 1993a) model atmosphere computed with solar abundances for all the elements was used in the SYNTHE code to generate a preliminary synthetic spectrum. The abundances in the synthetic spectrum were then modified to get agreement between observed and computed profiles of selected lines. The individual abundances estimated in that way were then used for computing an ATLAS12 model. This model and the measured equivalent widths of unblended lines with critically evaluated log gfs were the input data of the WIDTH code (Kurucz 1993a) which yields abundances from equivalent widths. A final ATLAS12 model computed for the average abundances derived from equivalent widths or, in a few cases, from line profiles, was the final input model used for computing the final synthetic spectrum. The final adopted abundances are listed in Table 1, column 3. They are logarithmic abundances relative to the total number of atoms N_{tot}. The second column of Table 1 shows the average abundances derived from the measured equivalent widths or from comparison of observed and computed profiles. Column 4 shows the solar abundances from Grevesse & Sauval (1998), where the scale $\log(N_{elem})$ relative to $\log(N_{\rm H})=12$ was changed to the scale $\log(N_{elem}/N_{\rm tot})$; col. 5 gives the over- or underabundance of the ions in HD 175640 relative to the solar abundances. The last column indicates whether lines lying shortward (UV) or longward (Vis) of the Balmer discontinuity (placed at $\lambda=$ 3647 Å) were used for the abundance determination. When both regions were used, the average abundance from each region is given in parentheses. The aim of this separation is to investigate the presence of vertical abundance stratifications. Each of the 57 ions considered for the analysis is extensively discussed in the Appendix A. Tables of the input and output line data for WIDTH can also be found in Appendix A (Tables A.1-A.3).

Fig. 1 compares the T-logτ_{ross} relation of the ATLAS9 and ATLAS12 models used for HD 175640. The He underabundance of HD 175640 is the main cause of the different temperature stratifications, in contrast with the statement of Norris (1971) that the helium abundance has little effect on the temperature structure. Abundances from the equivalent widths of Mn I and Mn II lines and of Fe I and Fe II lines did not indicate any need for a model parameter redetermination.

Starting from λ=5500 Å telluric absorptions were also approximately modelled by using telluric lines of the HITRAN database[3] converted into the SYNTHE format by Kurucz (1998, private communication). The computed telluric spectrum was simply superimposed on the observed and computed spectra without performing any instrumental broadening and convolution with the synthetic spectrum. The atlas is made up of the superimposed plots

[3] http://cfa-www.harvard.edu/HITRAN

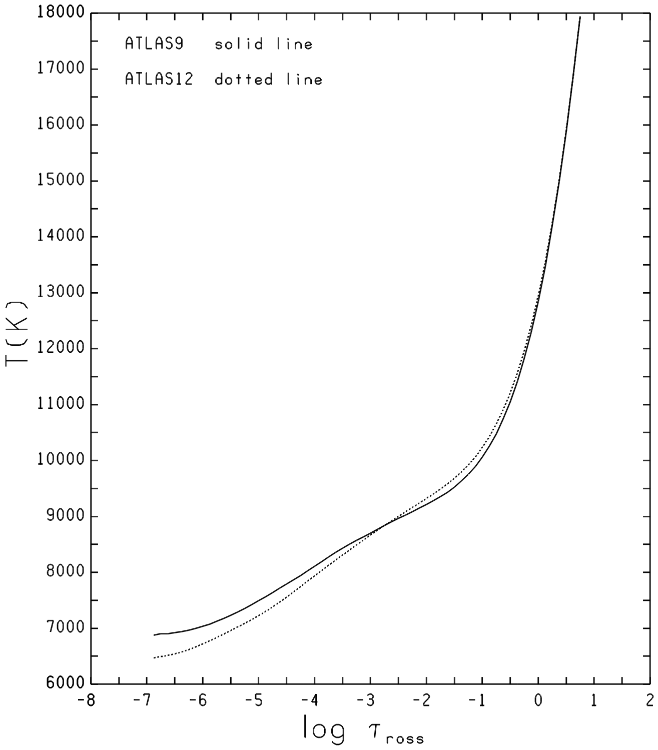

Fig. 1. The T-logτ_{ross} relation of an ATLAS9 model computed for solar abundances for all the elements (solid line) is compared with the T-logτ_{ross} relation of an ATLAS12 model computed with the individual abundances of HD 175640 (dotted line). Model parameters are $T_{\rm eff}$=12000 K, log g=3.95, ξ=0 km sec^{-1}.

of the observed spectrum, the computed stellar spectrum supplied with the line identifications, and the computed telluric spectrum.

4. Line Data

Atomic line lists from the Kurucz database[4] have provided the basis for the line data. They contain data mostly from the literature for light and heavy elements and computed by Kurucz (1992) for the iron group elements. In this case the critically evaluated transition probabilities from Martin, Fuhr & Wiese (1988) and Fuhr, Martin & Wiese (1988) were adopted for the lines in common. The files that we downloaded from the Kurucz website differ from those available in Kurucz & Bell (1995) for the Fe I line data.

We implemented the files gf0400.100, gf0500.100, gf0600.100, gf0800.100 and gf1200.100, which cover the range 3040-10000 Å, by replacing several log gfs with more up-to-date determinations and by adding missing lines, Stark broadening parameters, and hyperfine and isotopic components. In particular, we compared the line data of all the elements identified in HD 175640 on the basis of the Kurucz line lists with the line data from the

[4] http://kurucz.harvard.edu/linelists/gf100

Table 1. Abundances $\log(N_{elem}/N_{tot})$ for HD 175640.

	HD 175640		Sun		
	measured	adopted		[Element]	λ region
H		−0.008163	−0.036023		
He I	−1.73	−1.73	−1.11	[−0.62]	Vis
Be II	−10.64	−10.64	−10.64	[0.00]	UV
C I	−4.11±0.23	−4.00	−3.52	[−0.59]	Vis
C II	−4.05±0.16	−4.00	−3.52	[−0.53]	Vis
N I	≤−5.78	−5.78	−4.12	<[−1.66]	Vis
O I	−3.18±0.11	−3.18	−3.21	[+0.03]	Vis
Ne I	−4.35	−4.35	−3.96	[−0.39]	Vis
Na I	−5.47:	−5.47	−5.71	[+0.24]	Vis
Mg I	−4.64±0.06	−4.69	−4.46	[−0.18]	Vis
Mg II	−4.71±0.07	−4.69	−4.46	[−0.25]	Vis
Al I	<−7.50	−7.50	−5.57	<[−1.93]	Vis
Si II	−4.72±0.08	−4.71	−4.49	[−0.23]	Vis
Si III	−4.58±0.04	−4.71	−4.49	[−0.09]	Vis
P II	−6.28±0.08	−6.28	−6.59	[+0.31]	Vis
S II	−5.12±0.03	−5.12	−4.71	[−0.41]	Vis
Ca I	−5.26	−5.54	−5.68	[+0.42]	Vis
Ca II	−5.67±0.25	−5.54	−5.68	[+0.01]	UV(−5.83±0.06);Vis(−5.62±0.26)
Sc II	−9.08±0.15	−9.08	−8.87	[−0.21]	UV(−8.89±0.03);Vis(−9.21±0.08)
Ti II	−5.67±0.11	−5.67	−7.02	[+1.35]	UV(−5.59±0.09);Vis(−5.72±0.08)
V II	≤−9.04	−9.04	−8.04	<[−1.00]	UV
Cr I	−5.22±0.09	−5.36	−6.37	[+1.15]	UV(−5.18±0.05);Vis(−5.24±0.06)
Cr II	−5.41±0.07	−5.36	−6.37	[+0.96]	UV(−5.34±0.06);Vis(−5.41±0.07)
Mn I	−4.20±0.08	−4.20	−6.65	[+2.45]	UV(−4.22±0.08);Vis(−4.19±0.08)
Mn II	−4.25±0.04	−4.20	−6.65	[+2.40]	UV
Fe I	−4.78±0.08	−4.83	−4.54	[−0.24]	UV(−4.90±0.06);Vis(−4.75±0.05)
Fe II	−4.84±0.13	−4.83	−4.54	[−0.30]	Vis
Co II	−8.08:	−8.08	−7.12	[−0.96]:	UV
Ni II	−6.09±0.16	−6.09	−5.79	[−0.30]	UV(−6.01±0.13);Vis(−6.14±0.16)
Cu I	−6.52	−6.88	−7.83	[+0.95]	UV
Ga II	−5.43±0.04	−5.43	−9.16	[+3.73]	Vis
Br II	−7.12±0.04	−7.12	−9.41	[+2.29]	Vis
Sr II	−8.41	−8.41	−9.07	[+0.66]	Vis
Y II	−6.66±0.20	−6.66	−9.80	[+3.14]	UV(−6.42±0.06);Vis(−6.79±0.10)
Zr II	−8.67±0.17	−8.67	−9.44	[+0.77]	UV(−8.65±0.18);Vis(−8.78)
Rh II	−8.50:	−8.50	−10.92	[+2.42]:	UV
Pd I	−6.41±0.30	−6.41	−10.35	[+3.94]	UV
Xe II	−5.96±0.20	−5.96	−9.83	[+3.87]	Vis
Ba II	−9.27	−9.27	−9.91	[+0.64]	Vis
Pr III	−9.62:	−9.62	−11.33	[+1.71]:	Vis
Nd III	−9.57±0.08:	−9.60	−10.54	[+0.97]:	Vis
Yb II	−8.10±0.19	−8.10	−10.96	[+2.86]	UV(−7.82);Vis(−8.20±0.10)
Yb III	−7.31±0.01	−8.10	−10.96	[+3.66]	UV
Os II	−10.55:	−10.55	−10.55	[0.0]:	UV
Ir II	−10.65:	−10.65	−10.65	[0.0]:	UV
Pt II	−7.63	−7.63	−10.20	[+2.57]	Vis
Au II	−7.51±0.06	−7.51	−11.03	[+3.52]	Vis
Hg I	−6.19±0.18	−6.30	−10.91	[+4.72]	Vis
Hg II	−6.53±0.23	−6.30	−10.91	[+4.38]	Vis

NIST database[5] and from Wiese et al. (1996) for CNO. Generally, we preferred for our analysis NIST and Wiese et al. (1996) log gfs, although the differences with Kurucz's data are very small for most of the lines. We added several O I lines from Wiese et al. (1996), and a few Br II and several Xe II lines from NIST. We also examined other sources for specific elements like Si II (Lanz & Artru 1985), Ti II (Pickering et al. 2002), Cr II (Sigut & Landstreet 1990), Ga II (Isberg & Litzén 1985; Ryabchikova & Smirnov 1994;

[5] http://physics.nist.gov/cgi-bin/AtData/lines_form

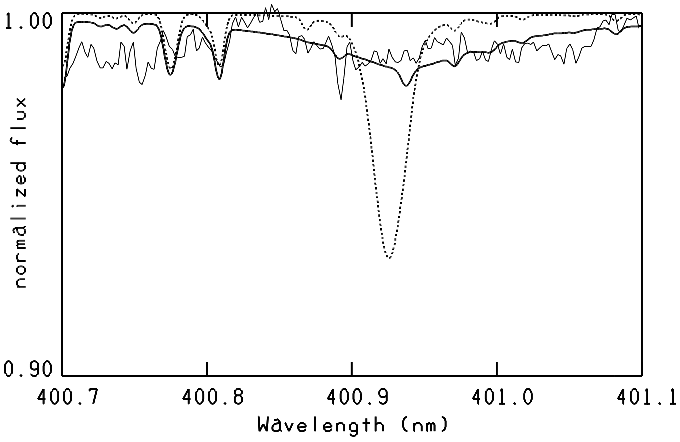

Fig. 2. Two synthetic profiles of He I 400.9257 nm differing only in the Stark damping constants are compared with the observations (full thin line). The thick line shows the profile computed with the Stark widths and shifts from Dimitrijević & Sahal-Bréchot (1990), the dotted line shows the profile computed with the approximate Stark damping constant yielded by the SYNTHE code (Kurucz & Avrett 1981) when it is not available from the literature. We used the model for HD 175640 having parameters $T_{\rm eff}$=12000 K, log g=3.95, microturbulent velocity ξ=0 km s^{-1}. The synthetic profiles are also broadened for v$sini$=2.5 km s^{-1} and for a gaussian instrumental profile with 110000 resolving power

Nielsen et al. 2000) , Y II (Nilsson et al. 1991), Xe II (Hansen & Persson 1987), Ce III(Biémont et al. 1999) , Pr III (Biémont et al. 2001b), Nd III (Zhang et al. 2002) , Yb II (Biémont et al. 1998), Yb III (Biémont et al. 2001a), Pt II (Dworetsky et al. 1984), Au II (Rosberg & Wyart 1997), Hg I (Benck et al. 1989) and Hg II (Sansonetti & Reader 2001; Proffitt et al. 1999). Actually, for the Rare Earth Elements we examined the DREAM database[6]

Because the Stark effect is an important line broadening mechanism in HD 175640 we also scrutinized the Stark line data. In the Kurucz line lists the damping constants $\gamma_S=4\pi$cw$/\lambda^2$ are taken from the literature when available. The Griem (1974) tables are the source for the damping constants of a large number of light element lines, while for all the lines of the iron group elements the damping constants are due to Kurucz's (1992) computations. The γ_S value for T=20000 K is that adopted in the line lists. We added Stark damping constants from Lanz, Dimitrijević & Artru (1988) for some Si II lines not considered by Griem (1974). Damping constants not available from the literature are computed inside the SYNTHE code with an approximate formula (Kurucz & Avrett 1981).

Lines of He I are computed separately. Stark profiles are given in tabular form as function of temperature, electron density and ion density for the He I lines at 4026 Å, 4387 Å, 4471 Å and 4922 Å. The Stark profiles for the first two lines were taken from Shamey (1969), those for the last two lines from Barnard, Cooper & Smith (1974) and Barnard, Cooper & Smith (1975), respectively. The Stark profile for the given model atmosphere is computed by interpolating in the tables. For some other He I lines, Stark profiles are obtained by interpolating for temperature the Stark widths and shifts taken from the Griem (1974) tables. For a few He I lines not available in Griem (1974) we added Stark widths and shifts computed by Dimitrijević & Sahal-Bréchot (1990) with a semiempirical approach. Fig. 2 compares two synthetic profiles for He I at 4009.26 Å predicted by the HD 175640 model atmosphere. They differ only in the Stark damping constant, which is computed according to the approximation made in the SYNTHE code in one case, and is derived from the Stark widths and shifts computed by Dimitijevic̀ & Sahal-Brèchot (1990) in the other case. This last profile agrees with the observed spectrum which is also plotted in Fig. 2. The large influence of the Stark effect, in spite of the weakness of the line, is evident from the figure.

Thanks to the very high resolution of the UVES spectra, isotopic shifts and hyperfine splittings are well detectable in several profiles, in particular those of Mn II, Ga II and Hg II. As a consequence, we may expect good agreement in their observed and computed profiles only when isotopic and hyperfine structures are taken into account in the computations. But these data are rather scarse in the literature, so that only few lines can be accurately computed. We included in the line list hyperfine components for some lines of Mn II (Holt et al. 1999); isotopic and hyperfine components for some lines of Ga II (Karlsson & Litzén 2000), Pt II (Engleman 1989), Hg I (Dolk et al. 2003), and Hg II (Dolk et al. 2003); isotopic components for Ba II at 4554.03 Å (Becker & Werth 1983; Becker et al. 1968). When the hyperfine components were not directly available in the literature, but only the A and B hyperfine constants were given, we used them in the HYPERFINE code (Kurucz & Bell 1995) for computing the hyperfine wavelengths and the corresponding hyperfine log gfs. Fig. 3 shows the extreme hyperfine broadening which affects the Mn II lines at 7353.549 Å and 7415.803 Å. In the figure each observed profile is compared with two synthetic profiles which differ in the hyperfine structure. One profile was computed by considering the hyperfine structure, the other profile was computed without it.

Isotopic and hyperfine components for Mn II, Ga II, Ba II, Hg I, and Hg II are discussed and listed in Appendix A (Tables A.6-A.9).

5. Discussion

The inspection of the atlas of HD 175640 shows a very large number of identified absorptions. The spectrum is crowded with Mn II, Mn I, Ti II and Cr II lines. In addition to H I, other identified species are He I, Be II, C I, C II, O I, O II, Ne I, Na I, Mg I, Mg II, Si II, Si III, P II, S I, S II, Ca I, Ca II, Sc II, Ti II, Cr I, Cr II, Mn I, Mn II, Fe I, Fe II, Co II(?), Ni II, Cu I, Ga I, Ga II, Br II, Sr II, Y II, Zr II, Rh II, Pd I, Xe II, Ba II, Pr III(?),Nd III(?), Yb II, Yb III, Os II(?),

[6] http://www.umh.ac.be/astro/dream.shtml

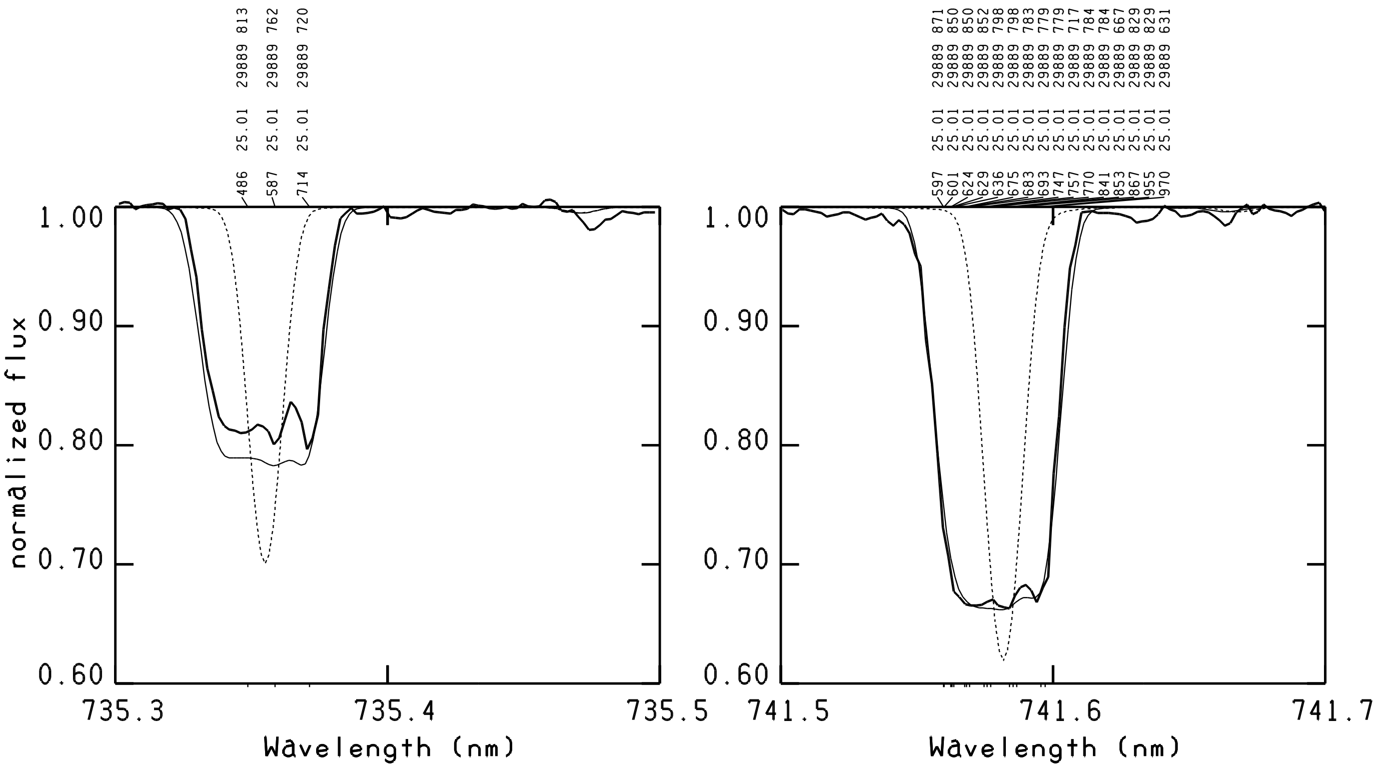

Fig. 3. The observed profiles (thick full lines) of Mn II at $\lambda\lambda$ 735.3549 and 741.5803 nm are compared with synthetic profiles computed once without any hyperfine structure (dotted lines) and once with hyperfine structure (thin full lines). The meaning of the line identification labels like 486 25.01 29889 813 is: 486, last 3 digits of wavelength in nm (735.3486); 25.01, element (25) and charge (01), i.e. Mn II; 29889, lower energy level in cm^{-1}; 813, per mil residual flux of the isolated line before rotation

Ir II(?), Pt II, Au II, Hg I and Hg II. Here, the question marks indicate doubtful identifications. A previous identification work in the range 3050-6750 Å based on the same spectrum studied by us was performed by Bord et al. (2003)[7] by using the wavelength coincidence statistics (WCS) method. They also identified Pd II which was missed by us (see Appendix A). The Bord et al. (2003) analysis as well as our atlas show that numerous features, in particular for λ>5000 Å, could not be identified. A list of unidentified lines in the range 4700-5800 Å is available in Appendix A (Table A.10). This region is approximately the same covered by the table of unanalyzed lines in HR 7775 in Wahlgren et al. (2000). The comparison of the two lists of unidentified lines has given a very small number of coincidences. In HD 175640, several unidentified absorptions coincide with lines of Mn II and Cr II having log gf values too low to yield a predicted profile of intensity similar to the observed one.

Numerous weak emission lines from Cr II and Ti II have been identified in the red part of the spectrum, starting at $\approx \lambda$ 5847 Å. They are all the Ti II lines with the lower excitation potential $> \sim 62000\,\mathrm{cm}^{-1}$ and log $gf > -1.0$ and all the Cr II lines with the lower excitation potential $> \sim 89000\,\mathrm{cm}^{-1}$ and log $gf > -0.8$. The observed emission lines of Ti II and Cr II are tabulated in Appendix A (Table A.4 and Table A.5) together with a few unidentified observed emission lines (Table A.11). Emission lines of C I at 9335.148 Å (mult. 10) and 9405.730 Å (mult. 9) have been observed for the first time. No clear Mn II emission lines were observed in HD 175640.

Considering the observational material at our disposal we notice that it is possible to identify different subgroups of HgMn stars on the basis of which ions appear in emission. 46 Aql (HD 186122) was the first HgMn star where emission lines of Mn II were detected (Sigut et al. 2000). Wahlgren & Hubrig (2000) found additional emission lines originating from the ions Fe II and Cr II. Emission lines of Mn II have further been found in HD 16727 and HD 41040. However, some other HgMn stars (e.g., HD 175640, HD 71066, HD 11073 or HD 178640) show exclusively Cr II and Ti II emission lines. The hypothesis has been made that the presence of emission lines of a particular element is correlated in some way with its abundance (Wahlgren & Hubrig 2000). Sigut (2001) explains the emission lines as due to NLTE effects interlocked with vertical stratified abundances of particular elements. However, there is also a group of HgMn stars which does not exhibit emission lines at all (e.g. HD 49606, HD 77350 or HD 78316). At the moment, the very small sample of HgMn stars with observed emission lines cannot answer the question of what excitation process leads to the weak emission lines. The proper identification and

[7] http://www.astro.lsa.umich.edu/users/cowley/AAS0503Don/P7143.htm

tabulation of emission lines in the spectrum of HD 175640 should help to advance and to test the theoretical explanation of their origin.

We can see in the atlas that unpredicted red components affect the K and H Ca II profiles at 3933 Å and 3968 Å and the Na I profiles at 5890 Å and 5896 Å. Their circumstellar or interstellar origin should be further investigated. An unexpected redshift of 0.2 Å for the Ca II profiles at 8498 Å and 8662 Å was explained by Castelli & Hubrig (2004) by an anomalous isotopic composition of Ca in HD 175640. The only other element in HD 175640 with an anomalous isotopic composition is Hg (Dolk et al. 2003).

Abundances for 49 ions from 40 elements (Table 1) were determined from both equivalent width and line profile analyses. The analysis of each ion is extensively discussed in Appendix A. The abundances for a number of ions (He I, C I-C II, O I, Na I, P II, S II, Ca I-Ca II, Sc II, Ti II, Br II, Sr II, Y II, Zr II, Rh II, Pd I, Xe II, Ba II, Nd III, Yb II-Yb III, Pt II and Au II) are reported here for the first time. The main interest in carrying out the abundance study of HD 175640 comes from the fact that no convincing explanation of the origin of HgMn stars presently exists and that the physical mechanisms producing observed abundance anomalies are not fully understood (e.g., Hubrig & Mathys 1995; Leckrone et al. 1999; Dolk et al. 2003). Abundance determinations from the analysis of stellar spectra play a critical and defining role for testing the several mechanisms that have been proposed to explain the development of the anomalies.

The examination of Table 1 shows that both excesses and deficiencies occur in the atmosphere. Compared to the solar abundance, Hg is the most overabundant element. It exceeds the solar abundance by a factor $> 10^4$. It is followed by Ga, Y, Pd, Xe, Yb III, and Au, which have abundances larger than the solar ones by factors of the order of 10^3. Mn, Br, Yb II, and Pt are overabundant by factors larger than 10^2, while Cr and Ti are overabundant by factors of the order of 10. Elements overabundant in a lesser degree are Cu ([+0.95]), Sr ([+0.66)], Zr ([0.77]), Ba ([+0.64]), and Nd ([+0.97]). The most underabundant elements are N, Al and V, which could not be identified in the spectrum, so that their underabundances of [−1.7], [−1.9] and [−1.0], respectively, are only upper limits. Other underabundant elements are He ([−0.62]), C ([−0.55]) and Co ([−0.96]). The abundances of the remaining elements lie within the limits of ± 0.5 dex

Only a few observational studies have been carried out to test the vertical abundance stratification of certain elements in HgMn stars (Alecian 1982; Lanz et al. 1993; Savanov & Hubrig 2003). Our study of HD 175640 revealed different abundances of singly ionized ions lying on either side of the Balmer jump. The differences are within the limits of the standard deviations for Ca II, Cr I, Cr II, Mn I, Ni II, Zr II. They are larger than the standard deviations for Sc II, Ti II, Fe I, Y II, and Yb II. In the near UV, these elements give abundances larger than those derived from the visual lines, except for Fe I for which the opposite is true.

Possible signs of an ionization anomaly have been found from the study of Cr I, Cr II and Yb II, Yb III lines. The average abundance obtained from lines of Cr II is lower by 0.2 dex than from lines of Cr I. For the REE Yb, we find that the average abundance from the Yb III lines is 0.8 dex higher than that from the Yb II lines. The 0.2 dex abundance difference from Cr I and Cr II lines seems to confirm the vertical Cr stratification inferred by Savanov & Hubrig (2003) from Cr II lines lying on the wings of H_β at different distances from the core, although they found the larger abundance difference of 0.6 dex. No sign of vertical Cr abundance stratification comes from the abundances of Cr I and Cr II lines lying on either side of the Balmer jump.

Finally, the synthetic spectrum analysis has shown some deficiencies of the UVES spectrum reduction procedures related to small uncertainties in the wavelength calibrations as well as to large jumps and undulations of the échelle spectra. All these shortcomings contribute to reducing the agreement of the computed spectra with the observed spectra in certain wavelength regions.

Acknowledgements. We would like to express our gratitude to M. Schöller for his help with the layout of the paper and the website.

References

Albayrak,B., Gulliver, A.F., Adelman, S.J., Aydin, C., Kocer, D. 2003, A&A 400, 1043
Alecian, G. 1982, A&A107, 61
Anders, E., Grevesse, N. 1989, Geochim. Cosmochim. Acta, 53, 197
Barnard, A.J., Cooper, J., Smith, E.W. 1974, J. Quant. Spect. Rad. Transfer 14, 1025
Barnard, A.J., Cooper, J., Smith, E.W. 1975, J. Quant. Spect. Rad. Transfer 15, 429
Becker, W., Werth, G. 1983, Z. Physik A 311, 41
Becker, W., Fisher, W., Huhnermann, H. 1968, Z. Physik 216, 142
Benck, E.C., Lawler, J.E., Dakin, J.T. 1989, J.Opt.Soc.Am. B, 6, 11
Berry, H.G., Bromander, J., Curtis, L.J., Buchta, R., 1971, Phys. Scr. 3, 125
Biémont, E., 1977, A&AS 27, 489
Biémont, E., Dutrieux, J.-F., Martin, I., Quintet, P. 1998, J.Phys. B.: At. Mol. Opt. Phys. 31, 3321
Biémont, E., Garnir, H.P., Lokhnygin, V., et al. 2001a, J.Phys. B: At. Mol. Opt. Phys. 34, 1869
Biémont, E., Garnir, H.P., Palmieri, P., et al. 2001b, Phys. Rev. A 64, 022503
Biémont, E., Grevesse, N., Kwiatkovski, M., Zimmermann, P. 1981, A&A 108, 127
Biémont, E., Palmieri, P., Quintet, P. 1999, Astrophys. Space Sci. 269-270, 635
Black, J.H., Wisheit, J.C., Laviana, E., 1972, ApJ 177, 567
Bord, D.J., Cowley, C.C., Norquist, P.L. 1997, MNRAS 284, 869

Bord, D.J., Cowley, C.R., Hubrig, S., Bidelman, W.P. 2003, AAS 202, 3210B
Castelli, F., Hubrig, S., 2004, A&A, 421L, 1
Corliss, C.H., Bozman, W.R. 1962, NBS Monograph 53
Cowley, C.R., Corliss, C.H. 1983, MNRAS 203, 651
Cowley, C., Wiese, W.L., Fuhr, J., Kuznetsova, L.A. 2000, Allen's astrophysical quantities, ed. A.N. Cox, 53
Dimitrijević, M.S., Sahal-Bréchot, S. 1990, A&AS 82, 519
Dolk, L., Wahlgren, G.M., Lumdberg, H. et al. 2002, A&A 385, 111
Dolk, L., Wahlgren, G.M., Hubrig, S. 2003, A&A 402, 299
Dworetsky, M.M., Budaj, J. 2000, MNRAS 318, 1264
Dworetsky, Men.M., Jomaron, C.M., Smith, C.A. 1998, A&A 333, 665
Dworetsky, M.M., Storey, P.J., Jacobs, J.M., 1984, Phys. Scr. T8, 39
Engleman, R. Jr., 1989, ApJ 340, 1140
Fuhr, J.R., Martin, G.A., Wiese, W.L. 1988, J. Phys. Chem. Ref. Data, 17, Suppl. 4
Grevesse, N., Sauval, A.J. 1998, Space Science Reviews 85, 161
Griem, H.R. 1974, Spectral Line Broadening by Plasmas, Academic Press
Gulliver, A.F., Adelman, S.J., Friesen, T,P., A&A 413, 285
Hannaford, P., Lowe, R.M., Grevesse, N., Biémont, E., Whaling, W. 1982, ApJ 261, 736
Hansen, J.E., Persson, W. 1987, Physica Scripta 36, 602
Heise, H., 1974, A&A 34, 275
Hempel, M., Holweger, H. 2003, A&A 408, 1065
Hibbert, A., 1988, Phys. Scr. 38, 37
Holt, R.A., Scholl, T.J., Rosner, S.D. 1999, MNRAS 306, 107
Hubrig, S., Castelli, F. 2001, A&A 375, 963
Hubrig, S., Castelli, F., Wahlgren, G.M. 1999, A&A 346, 139
Hubrig, S., Mathys, G. 1995, Comments on Astrophys. 18, 167
Isberg, B., Lizèn, U. 1985, Physica Scripta 31, 533
Johansson, S., Wallerstein, G., Gilroy, K.K., Joueizadeh, A. 1995, A&A 300, 521
Jomaron, C.M., Dworetsky, M.M., Allen, C.S. 1999, MNRAS 303, 555
Karlsson, H., Litzèn, U. 2000, J.Phys.B: At. Mol. Opt. Phys. 33, 2929
Kostyk, R.I, Orlova, T.V. 1983, Astrometrya Astrofiz. 49, 39
Kurucz, R.L., 1988, Trans. IAU, XXB, ed. M.McNally, Dordrecht: Kluwer, 168
Kurucz, R.L. 1992, Rev. Mexicana Astron. Astrof. 23, 45
Kurucz, R.L. 1993a, "ATLAS9 Stellar Atmosphere Programs and 2 km/s grid", CD-ROM, No 13
Kurucz, R.L. 1993b, "SYNTHE Spectrum Synthesis Programs and Line Data", CD-ROM, No 18
Kurucz, R.L. 1997, in The 3rd Conf. on Faint Blue Stars, eds. A.G.D. Philip, J. Liebert, & R.A. Saffer (L. Davis Press: Schenectady), 33
Kurucz, R.L., 2003, private communication
Kurucz, R.L., Avrett, E.H., 1981, Solar Spectrum Synthesis. I. A sample atlas from 224 to 300 nm, SAO Spec. Rep. 391
Kurucz, R.L., Bell, B. 1995, "Atomic Line List", CD-ROM No 23
Kurucz, R.L., Peytremann, E. 1975, SAO Special Report, 362
Lanz, T., Artru, M.-C., 1985, Phys. Scr. 32, 115
Lanz, T., Artru, M.C., Didelon, P., Mathys, G. 1993, A&A 272, 465
Lanz, T., Dimitrijević, Artru, M.C. 1988, A&A 192, 249
Leckrone, D.S., Proffitt, C.R., Wahlgren, G.M. et al. 1999, AJ 117, 1454
Martin, G.A., Fuhr, J.R., Wiese, W.L. 1988, J. Phys. Chem. Ref. Data, 17, Suppl. 3
Miles, B.M., Wiese, W.L. 1969, NBS Technical Note 474
Moore, C.E. 1965, Selected Tables of Atomic Spectra, NSRDS-NBS 3
Moore, C.E. 1972, A Multiplet Table of Astrophysical Interest, NSRDS-NBS 40
Nielsen, H., Karlsson, H., Wahlgren, G.M. 2000, A&A 363, 815
Nilsson, A.E., Johansson, S., Kurucz, R.L. 1991, Physica Scripta 44, 226
Norris, J. 1971, ApJS 23, 213
Pickering, J.C., Thorne, A.P., Perez, R. 2002, ApJS 138, 247
Proffitt, C.R., Brage, T., Leckrone, D.S. et al. 1999, ApJ 512, 942
Raassen, A.J.J., Uylings, P.H.M., 1998, A&A 340, 300; http://www.science.uva.nl/pub/orth/iron/FeII.E1
Rosberg, M., Wyart, J.-F. 1997, Physica Scripta 55, 690
Ryabchikova, T.A., Smirnov, YU. M. 1994, Astronomy Report 38, 70
Sadakane, K., Jugaku, J., Takada-Hidai, M. 1985, ApJ 297, 240
Sadakane, K., Jugaku, J., Takada-Hidai, M. 1988, ApJ 325, 776
Sadakane, K., Takada-Hidai, M., Takeda, Y., et al. 2001, PASJ 53, 1223
Sansonetti, C.J., Reader, J.,2001, Phys. Scr. 63, 219
Savanov, I., Hubrig, S. 2003, A&A 410, 299
Shamey, L.J. 1969, unpublished Ph.D. thesis, University of Colorado
Schulz-Gulde, E., 1969, JQRST 9, 13
Sigut, T.A.A. 2001, A&A 377, L27
Sigut, T.A.A., Landstreet, J.D., Shorlin, S.L.S. 2000, ApJ 530, L89
Sigut, T.A.A., Landstreet, J.D. 1990, MNRAS 247, 611
Smith, K.C. 1993, A&A 276, 393
Smith, K.C. 1994, A&A 291, 521
Smith, K.C. 1996, A&A 305, 902
Smith, K.C. 1997, A&A 319, 928
Smith, K.C., Dworetsky, M.M. 1993, A&A 274, 335
Wahlgren, G.M., Hubrig, S. 2000, A&A 362L, 13
Wahlgren, G.M., Dolk, L., Kalus, G., et al. 2000, ApJ 539, 908
Wiese, W.L., Fuhr, J.R., Deters, T.M. 1996, J. Phys. Chem. Ref. Data, Monograph 7
Wiese, W.L., Martin, G.A. 1980, NSRDS-NBS 68
Wiese, W.L., Smith, M.W., Glennon, B.M., 1966, NSRDS-NSB 4
Wujec, T., Weniger, J. 1981, J. Quant. Spectrosc. Radiat. Transfer 25, 167
Zhang, Z.G., Svanberg, S., Palmieri, P., Quintet, P., Biémont, E. 2002, A& 385, 724